

Copper-64 PET imaging of the CXCR4 chemokine receptor using a cross-bridged cyclam bis-tetraazamacrocyclic antagonist

Benjamin P. Burke^{1,2†}, Cecilia S. Miranda^{2,3†}, Rhiannon E. Lee^{1,2}, Isaline Renard^{1,2}, Shubhanchi Nigam^{2,3}, Gonçalo S. Clemente^{2,3}, Thomas D’Huys⁴, Torsten Ruest³, Juozas Domarkas^{1,2}, James A. Thompson^{2,5}, Timothy J. Hubin⁶, Dominique Schols⁴, Christopher J. Cawthorne^{2,3*}, Stephen J. Archibald^{1,2,3*}

¹Department of Chemistry, University of Hull, Cottingham Road, Hull, HU6 7RX, UK.

²Positron Emission Tomography Research Centre, University of Hull, Cottingham Road, Hull, HU6 7RX, UK

³Department of Biomedical Sciences, University of Hull, Cottingham Road, Hull, HU6 7RX, UK.

⁴Rega Institute for Medical Research, KU Leuven, Leuven, Belgium.

⁵Hull York Medical School (HYMS), University of Hull, Cottingham Road, Hull, HU6 7RX, UK.

⁶Department of Chemistry and Physics, Southwestern Oklahoma State University, Weatherford, OK 73096, USA.

ORCID ID: Cawthorne 0000-0002-5975-0354; Archibald 0000-0001-7581-8817

Running Title: Copper-64 PET imaging of CXCR4

Corresponding Author: *T: (+44)1482 465488; F: (+44)1482 466410; E: s.j.archibald@hull.ac.uk

First Author: T: (+44)1482 465418; F: (+44)1482 466410; E: b.burke@hull.ac.uk; Fellow.

†These authors contributed equally.

Disclosure Statement: No potential conflicts of interest relevant to this article exist.

ABSTRACT

Expression of the chemokine receptor chemokine C-X-C motif receptor 4 (CXCR4) plays an important role in cancer metastasis, autoimmune diseases and during stem cell based repair processes after stroke and myocardial infarction. Previously reported positron emission tomography (PET) imaging agents targeting CXCR4 suffer from either high non-specific uptake or only bind to the human form of the receptor. The objective of this study is to develop a high stability copper-64 labelled small molecule PET agent for imaging both human and murine CXCR4 chemokine receptors. **Methods:** Synthesis, radiochemistry, stability and radioligand binding assays were performed for the novel tracer ^{64}Cu -CuCB-Bicyclam. *In vivo* dynamic PET studies were carried out on mice bearing U87 (CXCR4^{low}) and U87.CXCR4 (CXCR4^{high}) tumors. Biodistribution and receptor blocking studies were carried out on CD1-IGS immunocompetent mice. CXCR4 expression on tumor and liver disaggregates was confirmed using a combination of immunohistochemistry, quantitative polymerase chain reaction (qPCR) and western blot. **Results:** ^{64}Cu -CuCB-Bicyclam has a high affinity for both the human and murine variants of the CXCR4 receptor ($\text{IC}_{50} = 8 \text{ nM}$ (human)/ 2 nM (murine)) and can be obtained from the parent chelator that has low affinity. *In vitro* and *in vivo* studies demonstrate specific uptake in CXCR4 expressing cells that can be blocked by >90% using a higher affinity antagonist, with limited uptake in non-CXCR4 expressing organs and high *in vivo* stability. The tracer was also able to selectively displace the CXCR4 antagonists AMD3100 and AMD3465 from the liver. **Conclusions:** The application of the tetraazamacrocyclic small molecule ^{64}Cu -CuCB-Bicyclam is demonstrated as an imaging agent

for the CXCR4 receptor that is likely to be applicable across a range of species. It has high affinity and stability and is suitable for preclinical research in immunocompetent murine models.

Keywords: CXCR4, copper-64, azamacrocyclic, cyclam, AMD3100.

INTRODUCTION

Chemokine C-X-C motif receptor 4 (CXCR4) is a seven-transmembrane helix G-protein coupled receptor. The interaction of CXCR4 with its cognate ligand, stromal cell-derived factor 1 α (SDF1- α / CXCL12), is essential during embryonic development and plays a key role in normal physiological function, including control of hematopoietic cells during homeostasis (1). CXCR4 is overexpressed in multiple cancer types, with expression levels associated with increased proliferation, migration and survival (2,3). In addition, CXCR4 expression on circulating tumor cells has been shown to enable metastasis to CXCL12 expressing organs including liver, lung and bone marrow (4) and inhibition of CXCR4-CXCL12 signalling reduces metastasis in various breast cancer models (5). There is a clear role in multiple myeloma, particularly in extra-medullary disease, a sub-type with poor prognosis that is chemotherapy resistant (6,7). Important links have been elucidated between CXCL12 and immunotherapies where blocking the signalling axis prevented recruitment of immunosuppressing fibroblast activation protein positive stromal cells (8). CXCR4 has also been shown to have a role in stroke, autoimmune disease (9,10) and myocardial infarction, with CXCL12 upregulated post-infarction (11-13). CXCR4 is therefore a candidate prognostic biomarker for a number of clinical indications; as a number of CXCR4 targeted agents are currently in clinical trials, it also has potential as a predictive biomarker to enable patient stratification.

The gallium-68 radiolabelled cyclic peptide CPCR4.2 (14,15), Pentixafor, has been used to demonstrate the potential of CXCR4 positron emission tomography (PET) imaging over the past few years. Pentixafor has been used clinically to image human CXCR4 expression in a range of

cancer types including, lymphoma, multiple melanoma, glioblastoma and small cell lung cancer in proof of concept studies (16-21). However, Pentixafor has little or no binding affinity to the murine variant of CXCR4 (18), limiting assessment of non-xenogenic CXCR4 expression in preclinical models.

Small molecule CXCR4 antagonists based on tetraazamacrocycles, including AMD3100 and AMD3465(22) (Supplemental Fig. 1), bind to both human and mouse variants of the receptor (23-26), with AMD3100 the sole CXCR4 antagonist currently US Food and Drug Administration and the European Medicines Agency approved for human use. The cyclam components of these molecules allow for transition metal complex formation, which switches the binding mode from electrostatic/ H-bonding between the protonated cyclam amine groups and aspartate residue side chains (171 and 262) to coordinate bonds with the same residues. Direct labelling with copper-64 to enable PET imaging has been attempted (27-30), and whilst CXCR4-dependent tumor uptake of ^{64}Cu -CuAMD3100 and ^{64}Cu -CuAMD3465 (Supplemental Fig. 1) has been demonstrated, high non-specific hepatic accumulation (likely caused by complex instability) prevented further development of these compounds (28,29). Copper(II) cyclam complexes are unlikely to have sufficient kinetic stability to retain the metal ion *in vivo* (31-38).

Configurational restriction of the cyclam with an ethylene cross-bridge confers kinetic stability on the copper(II) complex and increases affinity for/residence time at the CXCR4 receptor. The ethylene bridge in the macrocyclic rings of CB-bicyclam (Fig. 1B) allows only one configuration for the macrocycle copper(II) complex which optimises coordinate bond formation with CXCR4 residues relative to non-bridged cyclam metal complexes of AMD3100 (37,39-44).

The unbridged macrocycle complexes are in equilibrium between up to six possible configurations, leading to a stochastic overall affinity reflective of the average of these states. The affinity increase is likely mediated by reduction in bond lengths (effectively switched from axial to equatorial) to give shorter, stronger coordination bonds to CXCR4 receptor surface aspartate residues (39,40).

We have developed an understanding of structure activity relationships of CXCR4 binding bridged azamacrocyclic compound and set out to apply this knowledge to development of PET imaging probes. Currently, there are no blockable and stable nuclear imaging agents which bind to both human and non-human variants of CXCR4; inhibiting research in syngeneic models or understanding the role of CXCR4 in developmental pathways (45). In this work, we investigate a copper-64 labelled tetraazamacrocyclic small molecule CXCR4 antagonist, which has suitable characteristics (biodistribution, specificity and stability) for imaging both the human and murine homologues of the CXCR4 receptor.

MATERIALS AND METHODS

Ethics

All animal procedures were approved by the University of Hull Animal Welfare Ethical Review Body and carried out in accordance with the United Kingdom's Guidance on the Operation of Animals (Scientific Procedures) Act 1986 and the UKCCCR Guidelines 2010 (Home Office Project License number 60/4549) (46).

General

All chemicals were supplied by Sigma-Aldrich (UK) unless otherwise stated and used as supplied. Elemental analysis was performed using a CHN analyser EA1108 (Carlo Erba). Accurate mass spectrometry measurements were obtained using a LQT Orbitrap XL. Semi-preparative high performance liquid chromatography was carried out using an Agilent 1100 series equipped with a Ultraviolet light detector (series G1314A) and a NaI radiodetector. Thin layer chromatography was carried out using neutral alumina sheets (Merck USA), eluting with methanol 95:5 water, saturated with excess NaCl. Radio-TLC was carried out using a Lablogic ScanRam, equipped with a NaI detector at a speed of 10 mm/min. Data were recorded using Lablogic Laura (version 4.1.13.91). Copper-64 was purchased from the University of Cambridge. Further details of synthesis, radiochemistry and stability methodologies are present in the supplemental information (Supplemental Figs. 2 and 3). ^{64}Cu -CuAMD3100 was synthesized and analysed following the reported procedure (27).

Cell Lines

The U87 cell line was purchased from American Type Culture Collection, the glioblastoma astrocytoma U87.CD4 cell line was transfected with CXCR4 (human) or CXCR4 (murine). Both U87 and U87.CXCR4 (human and murine) cells were grown in Dulbecco's modified Eagle's medium with L-Glutamine medium (Lonza, Belgium) with U87.CXCR4 supplemented with 2 µg/ml puromycin. All cell lines were cultured in the presence of 10% foetal bovine serum, in a humidified incubator with 5% CO₂. The intracellular calcium mobilization in response to CXCL12 was measured in U87.CXCR4 (human) cell lines at 37°C by monitoring the fluorescence of an intracellular calcium probe (Fig. 1A) as a function of time using a Fluorometric Imaging Plate Reader (FLIPR; Molecular Devices, Sunnyvale USA) (40,47) with compounds (AMD3100, CuAMD3100, CB-Bicyclam, CuCB-Bicyclam, Cu₂CB-Bicyclam) tested in the concentration range 0.01-10,000 nM. Flow cytometry was carried out as previously described using a FACSCalibur (Becton Dickinson USA) and data were analysed using Cellquest software (39). CXCR4 expression was determined by western blot, immunohistochemistry (as previously described) (15,28) and quantitative polymerase chain reaction (qPCR) as previously described (Supplemental Table 1).

Receptor Binding Assay

U87.CXCR4 (human) cells grown to 60% to 80% confluence were used for receptor binding assays. Cells were washed with cold PBS buffer and flasks were placed on ice to prevent receptor internalization. Cells were detached using a cell scraper, centrifuged at 200 g for 5 minutes and then 5x10⁵ cells were resuspended with cold PBS buffer. Cells were incubated with 37 kBq/mL

(5.2 nM) of ^{64}Cu -CuCB-Bicyclam in PBS for 60 minutes at 4°C. After incubation, cells were washed quickly three times with cold PBS and cell-associated radioactivity was determined in using an automatic gamma counter (Wizard 3' Wallac, UK).

For blocking experiments, cells were preincubated with 20 μM of Cu₂CB-Bicyclam for 1 h prior to washing three times in cold PBS buffer and incubation with radiotracer as above. Data is expressed as % incubated dose (%) \pm SEM, representing the mean of three independent experiments with three internal repeats.

Animal Models

Female CD1-IGS (CrI: CD1 (IGS)) and CD1-Nude (CrI: *CD1-Foxn1^{Nu}*) mice (age 21-27 days; weight 20-25 g) were purchased from Charles River Laboratories. CD1-Nude mice were subcutaneously (s.c.) implanted with a 5×10^6 cells/100 μL suspension of U87/U87-human CXCR4 cells in Geltrex basement membrane in the upper flank, under anaesthesia. Tumor sizes were measured every 2 days using calipers, and tumor volume was determined by using the equation length*width*height (to give volume in mm^3).

PET/CT Imaging and Analysis

Dynamic whole body PET and CT images were acquired on the Sedecal SuperArgus 2R PET scanner (Sedecal, Spain). Mice were induced with 5% isoflurane/oxygen (v/v) anaesthesia before maintenance at 2%, using a flow rate of 1 L/min. Mice were cannulated in the tail vein using a bespoke catheter before being placed into an imaging cell where temperature and respiration were monitored (Minerve, France). ^{64}Cu -CuCB-Bicyclam (8.9 ± 3.2 MBq, 7.15 GBq/ μmol , 1.2 nmol)

was injected at the beginning of a 90 minute dynamic imaging sequence (10 frames: 3x 120 s, 1x 240 s, 4x 600 s and 2x 1200 s). Mice were maintained at 1% anaesthesia during scanning, with temperature and respiration monitored throughout. Following the PET scan, a CT image was acquired for anatomic co-registration (40 kV, 140 μ A, 360 projections, 8 shots).

For specificity studies, a separate group of mice were injected with a blocking dose of 5 mg/kg of Cu₂CB-Bicyclam administered intraperitoneally 60 minutes prior to injection of ⁶⁴Cu-CuCB-Bicyclam.

PET emission data were reconstructed using an 3D ordered subset expectation maximisation (OSEM3D) algorithm with corrections for randoms, scatter and attenuation. Data were analysed using AMIDE (48) and Vivoquant software (InVivo, Boston, USA), with regions of interest (ROI) drawn over tumors and various tissues to generate time activity curves. Standardized uptake values (SUV) were obtained after correction for injected dose and animal weight. Tumor and liver samples were taken at sacrifice and fixed in formalin/frozen in liquid nitrogen.

***Ex vivo* Biodistribution, Urine Stability and Blocking studies**

CD1-IGS mice were injected intra-peritoneally with 5 mg/kg of Cu₂CB-Bicyclam, CuCB-Bicyclam, AMD3100 or AMD3465 in saline. For control experiments, no blocking injection was given. At 60 minutes after blocking, mice were injected i.v. with ~740 kBq of ⁶⁴Cu-CuCB-Bicyclam (or ⁶⁴Cu-AMD3100) in the tail vein, and this stock solution was used to calibrate the automatic gamma counter (Wizard 3'' Wallac, UK). 90 minutes post- tracer injection, blood, brain, heart, plasma, muscle, lungs, thymus, bone, spleen, nose, kidney, liver and intestines were collected

after sacrifice and dissection. Radioactivity within tissue samples was counted using the automatic gamma counter and counts per minute for each tissue sample were normalized to the total injected dose of radioactivity and weight of tissue to give the radioactivity uptake as %ID/g. Before sacrifice, urine was collected and analysed using radio-TLC using the same QC method as during synthesis to determine stability (27).

Data Analysis

Tumor uptake between CXCR4^{high} and CXCR4^{low} expressing tumors was compared via unpaired two-tailed t-test. Tumor and liver uptake was compared in blocked and non-blocked animals via unpaired one-tailed t-test. P-values of < 0.05 were considered to be statistically significant.

RESULTS

Synthesis and Characterisation

The formation of the non-radioactive analogue CuCB-Bicyclam was carried out by reacting the previously described CB-Bicyclam with a stoichiometric amount of copper(II) acetate to form the mono-copper derivative, after which analytically pure samples were obtained using size exclusion chromatography (Supplemental Fig. 2). *In vitro* binding affinity of the mono-copper complex to both human and murine CXCR4 was determined via a CXCL12 stimulated calcium flux signalling assay and the IC₅₀ value was determined to be 8 nM (human CXCR4), whereas the free

chelator precursor CB-Bicyclam displayed no measurable activity in this assay ($>2 \mu\text{M}$) (Supplemental Fig. 4). Similar results were observed for murine CXCR4 with an IC_{50} value of 2 nM for CuCB-Bicyclam in murine CXCL12 binding assay (Supplemental Fig. 5).

Radiochemistry, Purification and Stability

Radiochemical synthesis of ^{64}Cu -CuCB-Bicyclam was carried out by heating CB-Bicyclam with preformed ^{64}Cu -Cu(OAc) $_2$ and monitoring via radio-TLC (Supplemental Fig. 3). Upon full incorporation (40-50 minutes) the crude complex was purified from excess CB-Bicyclam using semi-preparative HPLC to give decay corrected isolated radiochemical yields of $69 \pm 5\%$ with a total synthesis time of 120 minutes and a specific activity of $7.15 \text{ GBq}/\mu\text{mol}$. The LogP value was determined to be -2.38 ± 0.18 . ^{64}Cu -CuAMD3100 was synthesized and analysed following literature procedures (28). *In vitro* acid stability was measured to indicate comparative stability between tracers by incubating in 6 M HClO $_4$ for 3 hours at 37°C. Identical radio-TLC methods were used to those used to analyse the radiosynthesis process and stability values of $92 \pm 3\%$ and $9 \pm 5\%$ were determined for ^{64}Cu -CuCB-Bicyclam and ^{64}Cu -CuAMD3100 respectively.

Receptor Expression and ^{64}Cu -CuCB-Bicyclam Radioligand Binding *In Vitro*

CXCR4 surface expression levels were determined by fluorescence-activated cell sorting for U87 (human CXCR4^{low}) and U87.CXCR4 (human CXCR4^{high}) cells (4,000 vs 148,000 receptors/cell respectively) (Fig. 1). Radioligand binding experiments showed similar ratios to the expression level for the binding of the tracer (0.66 ± 0.56 and $20.22 \pm 5.78\%$ applied dose for U87

(CXCR4^{low}) and U87.CXCR4 (CXCR4^{high}) cells respectively) (Fig. 1). Pre-incubation of U87.CXCR4 (CXCR4^{high}) cells with Cu₂CB-Bicyclam (IC₅₀ = 3 nM) decreased binding of ⁶⁴Cu-CuCB-Bicyclam by 89%, consistent with high specific uptake.

PET/CT Studies on Tumor Bearing Mice

Dynamic PET/CT studies carried out on U87 (human CXCR4^{low}) and U87.CXCR4 (human CXCR4^{high}) xenograft-bearing mice demonstrated significantly higher uptake in human CXCR4^{high} vs CXCR4^{low} tumors after administration of ⁶⁴Cu-CuCB-Bicyclam (9.6 ± 0.7 MBq), with SUV_{max} values of 7.36 ± 1.77% vs. 0.80 ± 0.14% at 80-90 minutes post-injection (Fig. 2). Tumor-to-muscle ratios at 90 min after injection were 23.6 ± 2.7 for U87.CXCR4 (CXCR4^{high}) and 3.0 ± 0.5 for U87 (CXCR4^{low}) tumors. Uptake was also seen in the kidneys and liver. Pre-injection of 10 mg/kg Cu₂-CB-Bicyclam 60 minutes before scanning reduced U87.CXCR4 (CXCR4^{high}) tumor and liver uptake by >90%. See Supplemental Figures 6 and 7 for all scan data and further analysis.

Ex Vivo Analysis of CXCR4 Expression

CXCR4 expression in U87.CXCR4 (CXCR4^{high}) and U87 (CXCR4^{low}) tumors and murine liver was confirmed *ex vivo* by a combination of western blot, immunohistochemistry and qPCR (Supplemental Fig. 8; Supplemental Table 1).

Biodistribution and Tracer Stability Studies in Immunocompetent Mice

Biodistribution studies were carried out using CD1-IGS mice at 90 minutes to determine the effect of a functional immune system on tracer distribution (Fig.3). Low uptake (<2 %ID/g) was noted in all organs except kidney (8.11 %ID/g) and organs known to express CXCR4 (spleen (4.71 %ID/g), lung (2.89 %ID/g) and liver (13.77 %ID/g)). Urine was analysed from a separate cohort of animals injected with ^{64}Cu -CuCB-Bicyclam and ^{64}Cu -CuAMD3100 pre-sacrifice. ^{64}Cu -CuCB-Bicyclam was >90% intact whilst only <10% of ^{64}Cu -CuAMD3100 remained intact in the urine.

Using murine liver CXCR4-dependent uptake of ^{64}Cu -CuCB-Bicyclam as a readout, the *in vivo* affinities/ residence times of Cu₂CB-Bicyclam, CuCB-Bicyclam, AMD3100 and AMD3465 were compared. Doses were administered 60 minutes prior to tracer administration and animals were sacrificed at several timepoints post-injection to provide tissue for biodistribution. Consistent with PET imaging in CD-1 Nude mice, pre-dosing with the Cu₂CB-Bicyclam significantly reduced tracer uptake in liver (3.40 vs 13.77 %ID/g, $p<0.05$), spleen (0.48 vs 4.71 %ID/g, $p<0.01$) and lungs (1.06 vs 2.89 %ID/g, $p<0.05$) at 60 minutes but not 12 hours; similar results were seen using CuCB-Bicyclam. No significant decrease in liver uptake was seen when animals were pre-injected with AMD3100 or AMD3465 at any timepoint.

DISCUSSION

This study reports a high-affinity CXCR4-specific PET imaging agent (^{64}Cu -CuCB-Bicyclam) which binds selectively and with high stability to both human and murine variants of the CXCR4 receptor. Although ^{64}Cu -CuCB-Bicyclam has potential as a clinical diagnostic PET imaging agent for oncology, it also represents a useful tool for the interrogation of CXCR4 expression levels over time in genetically engineered/immunocompetent pre-clinical models, useful in the investigation of CXCR4 targeting synergy with immunomodulatory therapies (49).

Unlike AMD3100 and AMD3465, the labelling precursor CB-Bicyclam has CXCR4 affinity of $> 2 \mu\text{M}$ due to the alkylation of the secondary amines disrupting the hydrogen bonding potential. The mono-copper species CuCB-Bicyclam has a higher affinity to the CXCR4 receptor than both AMD3100 and CuAMD3100 but lower than our previously described bis-copper species (Cu_2CB -Bicyclam). However, it is likely to be sufficient for imaging studies and has the advantage of a precursor with >100 fold lower receptor affinity. Copper-64 radiolabelling was carried out using the minimum concentration required for full radiometal incorporation. We chose to purify ^{64}Cu -CuCB-Bicyclam from unreacted CB-Bicyclam using semi-prep HPLC for these experiments.

Radioligand binding experiments using U87.CXCR4 ($\text{CXCR4}^{\text{high}}$) and U87 ($\text{CXCR4}^{\text{low}}$) cells showed specific binding, with binding correlating well with quantified surface expression levels of CXCR4. In addition, *in vitro* binding could be blocked using the higher affinity complex Cu_2CB -Bicyclam. *In vivo* PET/CT imaging using human CXCR4 U87.CXCR4 ($\text{CXCR4}^{\text{high}}$) and U87 ($\text{CXCR4}^{\text{low}}$) tumor-bearing mice mirrored the *in vitro* binding results, with selective high uptake in $\text{CXCR4}^{\text{high}}$

tumors at 90 minutes post-injection. *In vivo* specificity was confirmed using a blocking dose of the higher affinity Cu₂CB-Bicyclam, which reduced CXCR4^{high} tumor uptake by >90%.

As seen in previous studies utilising copper-64 labelled macrocycles for CXCR4 imaging, moderate liver uptake was seen on PET imaging using ⁶⁴Cu-CuCB-Bicyclam. This uptake was reduced after blocking with Cu₂CB-Bicyclam (5 mg/kg) to a comparable extent as that of CXCR4^{high} tumors, suggesting specific binding to CXCR4. This compares to previous studies, where very high doses of AMD3100 (50 mg/kg) were used for blocking (33). Murine liver expression of CXCR4 was confirmed after *ex vivo* disaggregation of tumor or liver at the protein level via FACS and immunohistochemistry. Further experiments demonstrated that >90% of urine radioactivity was intact ⁶⁴Cu-CuCB-Bicyclam, whereas the majority of activity from ⁶⁴Cu-CuAMD3100 injected animals was in the form of free copper-64 ions. Acid stability assays (6 M HClO₄) showed similar profiles for stability. These data are consistent with *in vitro* studies, demonstrating that cyclam copper(II) complexes which do not possess either structural reinforcement or coordinating arms have rapid binding kinetics but low stability in competition experiments (31,50,51). This data confirms both the insufficient stability of any non-bridged/ non-functionalized cyclam based copper(II) complex for *in vivo* PET imaging applications and also the higher stability of cross-bridged cyclam structures.

Further biodistribution studies were carried out using immunocompetent mice, to study the effect of blocking with various CXCR4 antagonists on the uptake of ⁶⁴Cu-CuCB-Bicyclam. As expected, liver uptake of the tracer could be blocked by administration of either the higher affinity Cu₂CB-Bicyclam or CuCB-Bicyclam at 60 minutes prior to tracer administration. However,

tracer uptake could not be blocked by the lower affinity CXCR4 antagonists; AMD3100 and AMD3465 (Fig. 3 and Supplemental Table 2). This could be explained by shorter (i.e. < 60 minute) receptor residence times for the unbridged cyclam compounds and/or displacement of AMD3100 or AMD3465 from CXCR4 by the higher affinity ⁶⁴Cu-CuCB-Bicyclam compound (30). Whilst the development of therapeutic agents targeting CXCR4 was not the focus of this study, the high stability, high affinity and appropriate biodistribution of ⁶⁴Cu-CuCB-Bicyclam makes the exploration of the identical radioactive and non-radioactive analogues as an imaging/chemotherapeutic pair of interest. The copper-67 derivative is of interest to investigate a radionuclide theranostic approach (52), assuming that the CXCR4 related liver uptake in humans is lower than in mice.

CONCLUSION

In this study we have developed a copper-64 labelled configurationally restricted azamacrocyclic CXCR4 antagonist with high affinity and stability and with favourable biodistribution characteristics. ⁶⁴Cu-CuCB-Bicyclam is the first CXCR4 targeted PET imaging agent, with suitable characteristics for routine imaging studies, which binds to both the human and murine CXCR4 receptor variants. This allows wider pre-clinical assessment of the role of CXCR4 in syngeneic tumor models and in immunocompetent models. It will also be useful for translation to other animal models of disease where imaging of the endogenous CXCR4 receptor is required.

ACKNOWLEDGEMENTS

We gratefully acknowledge the Daisy Appeal Charity for funding (Grant: DAhul0211 and BPB fellowship), Yorkshire Cancer Research (HEND376) and Dr Assem Allam and his family. REL and CSM would like to thank the University of Hull for studentship funding. Mass spectrometry data was acquired at the EPSRC UK National Mass Spectrometry Facility at Swansea University.

KEY POINTS

Question: The goal of this study is to develop a configurationally restricted azamacrocyclic compound as a high affinity and high stability copper-64 radiotracer for imaging CXCR4 chemokine receptor expression in mice and in humans.

Pertinent Findings: The radiotracer ^{64}Cu -CuCB-Bicyclam binds with high affinity to both murine and human CXCR4. The compound retains the copper-64 radiolabel and is excreted intact, with blocking studies *in vivo* showing significant reduction in uptake in liver, spleen and human CXCR4 expressing tumour.

Translational implications: ^{64}Cu -CuCB-Bicyclam is an appropriate tracer for studies of murine CXCR4 expression in mouse models and can be translated for use in humans.

REFERENCES

1. Zou YR, Kottmann AH, Kuroda M, Taniuchi I, Littman DR. Function of the chemokine receptor CXCR4 in haematopoiesis and in cerebellar development. *Nature*. 1998;393:595-599.
2. Balkwill F. The significance of cancer cell expression of the chemokine receptor CXCR4. *Semin Cancer Biol*. 2004;14:171-179.
3. Yoon Y, Liang ZX, Zhang Y, et al. CXC chemokine receptor-4 antagonist blocks both growth of primary tumor and metastasis of head and neck cancer in xenograft mouse models. *Cancer Res*. 2007;67:7518-7524.
4. Burger JA, Kipps TJ. CXCR4: a key receptor in the crosstalk between tumor cells and their microenvironment. *Blood*. 2006;107:1761-1767.
5. Singh B, Cook KR, Martin C, et al. Evaluation of a CXCR4 antagonist in a xenograft mouse model of inflammatory breast cancer. *Clin Exp Metastasis*. 2010;27:233-240.
6. Nervi B, Ramirez P, Rettig MP, et al. Chemosensitization of acute myeloid leukemia (AML) following mobilization by the CXCR4 antagonist AMD3100. *Blood*. 2009;113:6206-6214.
7. Roccaro AM, Mishima Y, Sacco A, et al. CXCR4 regulates extra-medullary myeloma through epithelial-mesenchymal-transition-like transcriptional activation. *Cell Rep*. 2015;12:622-635.
8. Feig C, Jones JO, Kraman M, et al. Targeting CXCL12 from FAP-expressing carcinoma-associated fibroblasts synergizes with anti-PD-L1 immunotherapy in pancreatic cancer. *Proc Natl Acad Sci U S A*. 2013;110:20212-20217.
9. Hummel S, Van Aken H, Zarbock A. Inhibitors of CXC chemokine receptor type 4: putative therapeutic approaches in inflammatory diseases. *Curr Opin Hematol*. 2014;21:29-36.
10. Ruscher K, Kuric E, Liu YW, et al. Inhibition of CXCL12 signaling attenuates the postischemic immune response and improves functional recovery after stroke. *J Cereb Blood Flow Metab*. 2013;33:1225-1234.
11. Ghadge SK, Muhlstedt S, Ozcelik C, Bader M. SDF-1 alpha as a therapeutic stem cell homing factor in myocardial infarction. *Pharmacol Ther*. 2011;129:97-108.
12. Kitaori T, Ito H, Schwarz EA, et al. Stromal cell-derived factor 1/CXCR4 signaling is critical for the recruitment of mesenchymal stem cells to the fracture site during skeletal repair in a mouse model. *Arthritis Rheum*. 2009;60:813-823.

13. Kucia M, Dawn B, Hunt G, et al. Cells expressing early cardiac markers reside in the bone marrow and are mobilized into the peripheral blood after myocardial infarction. *Circul Res*. 2004;95:1191-1199.
14. Demmer O, Gourni E, Schumacher U, Kessler H, Wester H-J. PET imaging of CXCR4 receptors in cancer by a new optimized ligand. *ChemMedChem*. 2011;6:1789-1791.
15. Gourni E, Demmer O, Schottelius M, et al. PET of CXCR4 expression by a Ga-68-labeled highly specific targeted contrast agent. *J Nucl Med*. 2011;52:1803-1810.
16. Herrmann K, Lapa C, Wester HJ, et al. Biodistribution and radiation dosimetry for the chemokine receptor CXCR4-targeting probe Ga-68-Pentixafor. *J Nucl Med*. 2015;56:410-416.
17. Philipp-Abbrederis K, Herrmann K, Knop S, et al. In vivo molecular imaging of chemokine receptor CXCR4 expression in patients with advanced multiple myeloma. *EMBO Mol Med*. 2015;7:477-487.
18. Wester HJ, Keller U, Schottelius M, et al. Disclosing the CXCR4 expression in lymphoproliferative diseases by targeted molecular imaging. *Theranostics*. 2015;5:618-630.
19. Lapa C, Luckerath K, Kleinlein I, et al. Ga-68-Pentixafor-PET/CT for imaging of chemokine receptor 4 expression in glioblastoma. *Theranostics*. 2016;6:428-434.
20. Lapa C, Luckerath K, Rudelius M, et al. Ga-68 Pentixafor-PET/CT for imaging of chemokine receptor 4 expression in small cell lung cancer - initial experience. *Oncotarget*. 2016;7:9288-9295.
21. Vag T, Gerngross C, Herhaus P, et al. First experience with chemokine receptor CXCR4-targeted PET imaging of patients with solid cancers. *J Nucl Med*. 2016;57:741-746.
22. Woodard LE, De Silva RA, Azad BB, et al. Bridged cyclams as imaging agents for chemokine receptor 4 (CXCR4). *Nucl Med Biol*. 2014;41:552-561.
23. Wong RSY, Bodart V, Metz M, Labrecque J, Bridger G, Fricker SP. Comparison of the potential multiple binding modes of bicyclam, monocyclam, and noncyclam small-molecule CXC chemokine receptor 4 inhibitors. *Mol Pharmacol*. 2008;74:1485-1495.
24. Bodart V, Anastassov V, Darkes MC, et al. Pharmacology of AMD3465: A small molecule antagonist of the chemokine receptor CXCR4. *Biochem Pharmacol*. 2009;78:993-1000.

25. De Clercq E. Recent advances on the use of the CXCR4 antagonist plerixafor (AMD3100, Mozobil (TM)) and potential of other CXCR4 antagonists as stem cell mobilizers. *Pharmacol Ther.* 2010;128:509-518.
26. Debnath B, Xu SL, Grande F, Garofalo A, Neamati N. Small molecule inhibitors of CXCR4. *Theranostics.* 2013;3:47-75.
27. Jacobson O, Weiss ID, Szajek L, Farber JM, Kiesewetter DO. ⁶⁴Cu-AMD3100 - A novel imaging agent for targeting chemokine receptor CXCR4. *Bioorg Med Chem.* 2009;17:1486-1493.
28. Nimmagadda S, Pullambhatla M, Stone K, Green G, Bhujwala ZM, Pomper MG. Molecular imaging of CXCR4 receptor expression in human cancer xenografts with [⁶⁴Cu]AMD3100 positron emission tomography. *Cancer Res.* 2010;70:3935-3944.
29. De Silva RA, Peyre K, Pullambhatla M, Fox JJ, Pomper MG, Nimmagadda S. Imaging CXCR4 expression in human cancer xenografts: Evaluation of monocyclam Cu-64-AMD3465. *J Nucl Med.* 2011;52:986-993.
30. Weiss ID, Jacobson O, Kiesewetter DO, et al. Positron emission tomography imaging of tumors expressing the human chemokine receptor CXCR4 in mice with the use of ⁶⁴Cu-AMD3100. *Mol Imaging Biol.* 2012;14:106-114.
31. Boswell CA, Sun XK, Niu WJ, et al. Comparative in vivo stability of copper-64-labeled cross-bridged and conventional tetraazamacrocyclic complexes. *J Med Chem.* 2004;47:1465-1474.
32. Hubin TJ, McCormick JM, Collinson SR, Alcock NW, Busch DH. Ultra rigid cross-bridged tetraazamacrocycles as ligands - the challenge and the solution. *Chem Commun.* 1998:1675-1676.
33. Lewis EA, Boyle RW, Archibald SJ. Ultrastable complexes for in vivo use: a bifunctional chelator incorporating a cross-bridged macrocycle. *Chem Commun.* 2004:2212-2213.
34. Mewis RE, Archibald SJ. Biomedical applications of macrocyclic ligand complexes. *Coord Chem Rev.* 2010;254:1686-1712.
35. Silversides JD, Allan CC, Archibald SJ. Copper(II) cyclam-based complexes for radiopharmaceutical applications: synthesis and structural analysis. *Dalton Trans.* 2007:971-978.
36. Silversides JD, Smith R, Archibald SJ. Challenges in chelating positron emitting copper isotopes: tailored synthesis of unsymmetric chelators to form ultra stable complexes. *Dalton Trans.* 2011;40:6289-6297.

37. Sun XK, Wuest M, Weisman GR, et al. Radiolabeling and in vivo behavior of copper-64-labeled cross-bridged cyclam ligands. *J Med Chem.* 2002;45:469-477.
38. Woodin KS, Heroux KJ, Boswell CA, et al. Kinetic inertness and electrochemical behavior of copper(II) tetraazamacrocyclic complexes: Possible implications for in vivo stability. *Eur J Inorg Chem.* 2005:4829-4833.
39. Khan A, Nicholson G, Greenman J, et al. Binding optimization through coordination chemistry: CXCR4 chemokine receptor antagonists from ultrarigid metal complexes. *J Am Chem Soc.* 2009;131:3416-3417.
40. Maples RD, Cain AN, Burke BP, et al. Aspartate-based CXCR4 chemokine receptor binding of cross-bridged tetraazamacrocyclic copper(II) and zinc(II) complexes. *Chem Eur J.* 2016;22:12916-12930.
41. McRobbie G, Valks GC, Empson CJ, et al. Probing key coordination interactions: configurationally restricted metal activated CXCR4 antagonists. *Dalton Trans.* 2007:5008-5018.
42. Smith R, Huskens D, Daelemans D, et al. CXCR4 chemokine receptor antagonists: nickel(II) complexes of configurationally restricted macrocycles. *Dalton Trans.* 2012;41:11369-11377.
43. Valks GC, McRobbie G, Lewis EA, et al. Configurationally restricted bismacrocylic CXCR4 receptor antagonists. *J Med Chem.* 2006;49:6162-6165.
44. Liang XY, Weishaupl M, Parkinson JA, Parsons S, McGregor PA, Sadler PJ. Selective recognition of configurational substates of zinc cyclam by carboxylates: Implications for the design and mechanism of action of anti-HIV agents. *Chem Eur J.* 2003;9:4709-4717.
45. Weiss ID, Jacobson O. Molecular imaging of chemokine receptor CXCR4. *Theranostics.* 2013;3:76-84.
46. Workman P, Aboagye EO, Balkwill F, et al. Guidelines for the welfare and use of animals in cancer research. *Br J Cancer.* 2010;102:1555-1577.
47. Princen K, Hatse S, Vermeire K, De Clercq E, Schols D. Evaluation of SDF-1/CXCR4-induced Ca²⁺ signaling by fluorometric imaging plate reader (FLIPR) and flow cytometry. *Cytometry Part A.* 2003;51A:35-45.
48. Loening AM, Gambhir SS. AMIDE: a free software tool for multimodality medical image analysis. *Mol Imaging.* 2003;2:131-137.

49. D'Alterio C, Nasti G, Polimeno M, et al. CXCR4-CXCL12-CXCR7, TLR2-TLR4, and PD-1/PD-L1 in colorectal cancer liver metastases from neoadjuvant-treated patients. *Oncoimmunology*. 2016;5:e1254313.
50. Wadas TJ, Wong EH, Weisman GR, Anderson CJ. Copper chelation chemistry and its role in copper radiopharmaceuticals. *Curr Pharm Des*. 2007;13:3-16.
51. Wei L, Ye Y, Wadas TJ, et al. Cu-64-Labeled CB-TE2A and diamsar-conjugated RGD peptide analogs for targeting angiogenesis: comparison of their biological activity. *Nucl Med Biol*. 2009;36:277-285.
52. Blower PJ. A nuclear chocolate box: the periodic table of nuclear medicine. *Dalton Trans*. 2015;44:4819-4844.

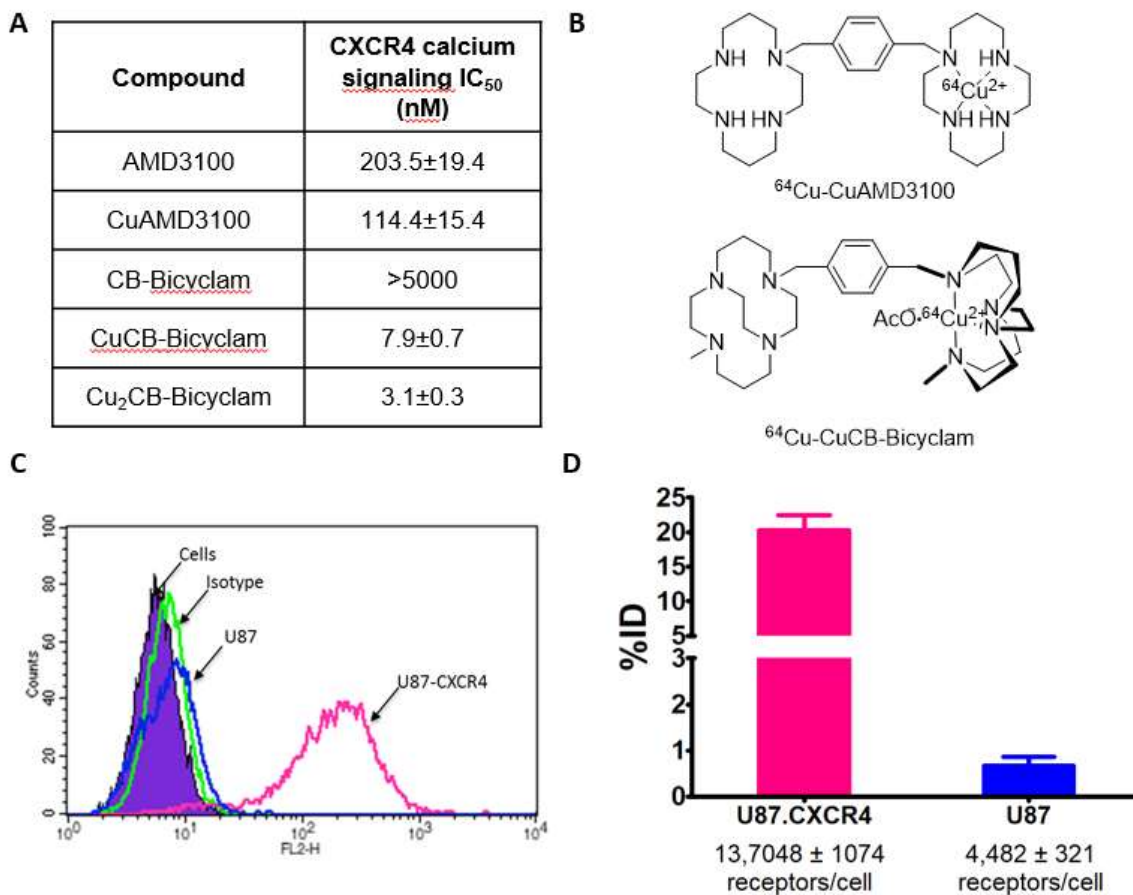


Figure 1 - In vitro assessment of ⁶⁴Cu-CuCB-Bicyclam (A) Comparative affinity values vs. CXCL12 determined by calcium flux assay, (B) Chemical structures of ⁶⁴Cu-CuAMD3100 and ⁶⁴Cu-CuCB-Bicyclam (C) FACS determination of CXCR4 expression and (D) Binding of ⁶⁴Cu-CuCB-Bicyclam on U87 (human CXCR4^{low}) and U87.CXCR4 (human CXCR4^{high}) expressing cell lines.

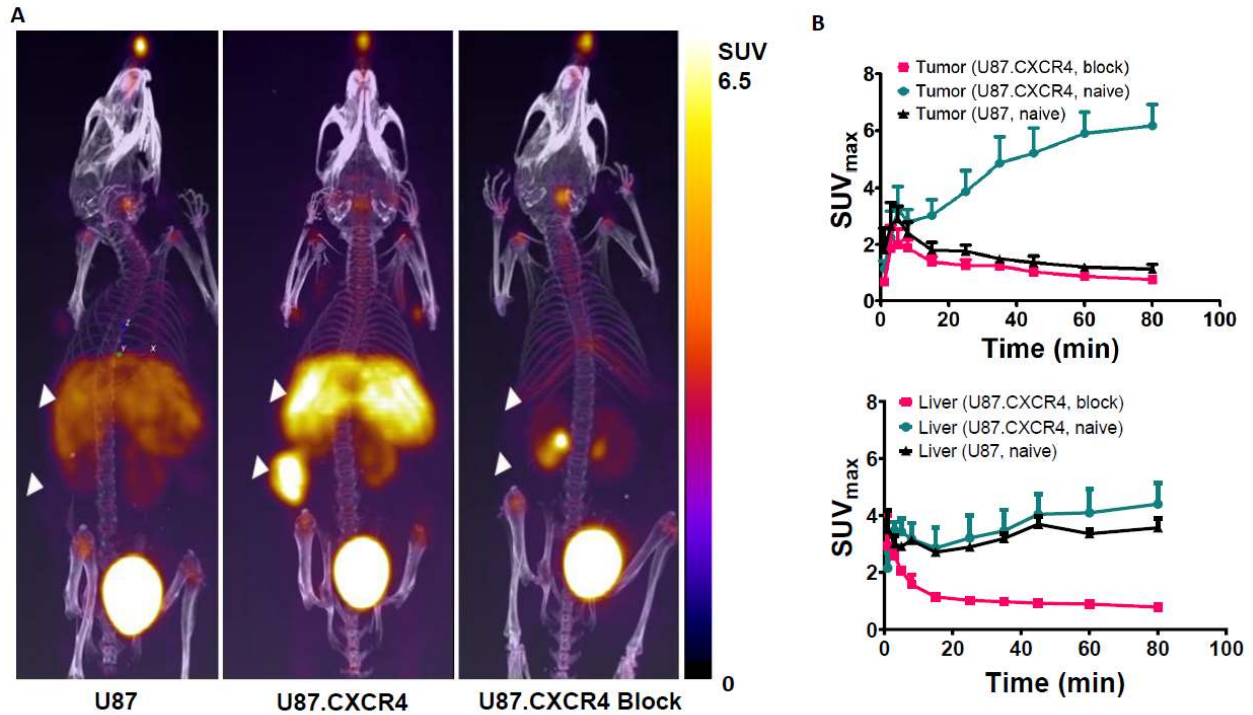


Figure 2 – In vivo PET/CT evaluation of ^{64}Cu -CuCB-Bicyclam. (A) Fused PET-CT maximum intensity projections at 70-90 mins post-injection from CD1 mice bearing U87-CXCR4 ($n=3$), U87 ($n=3$) and U87.CXCR4 block ($n=2$). Animals were injected with 9.6 ± 0.7 MBq of ^{64}Cu -CuCB-Bicyclam. Blocking dose of 5 mg/Kg of Cu₂CB-Bicyclam given 1 hour prior to ^{64}Cu -CuCB-Bicyclam injection where indicated. Arrows denote position of tumor and liver. (B) Dynamic tumor time activity for showing uptake of ^{64}Cu -CuCB-Bicyclam in tumor (top) and liver (bottom) during 90 minutes. Data represent mean uptake of $n=2-3$ animals \pm SEM. * U87.CXCR4 vs U87, $P<0.01$; **Block vs naïve, $P<0.01$. See Supplemental Figure 6 and 7 for all images at 70-90 mins and time activity curves for bladder, kidney and vena cava.

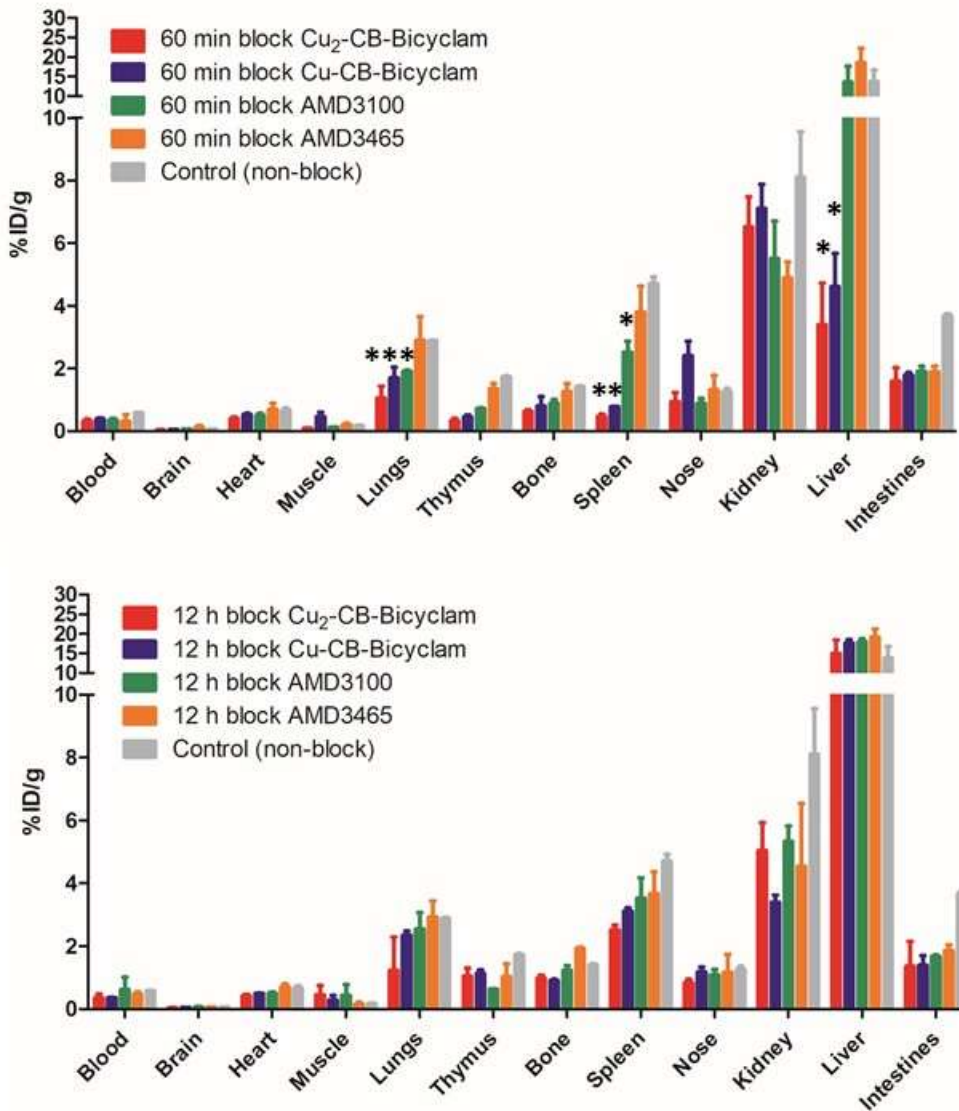


Figure 3 - Assessment of in vivo uptake of ⁶⁴Cu-CuCB-Bicyclam after blocking with a range of CXCR4 antagonists. Biodistribution of selected tissues from CD1-IGS mice pre-administered with 5 mg/Kg of Cu₂CB-Bicyclam, CuCB-Bicyclam, AMD3100 or AMD3465 60 minutes (top) and 12 hours (bottom) before ⁶⁴Cu-CuCB-Bicyclam injection. Tissue was harvested 90 minutes after tracer administration (n=4). *Block vs naïve, P<0.05



The Journal of
NUCLEAR MEDICINE

Copper-64 PET imaging of the CXCR4 chemokine receptor using a cross-bridged cyclam bis-tetraazamacrocyclic antagonist

Ben Burke, Cecilia Miranda, Rhiannon Lee, Isaline Renard, Shubhanchi Nigam, Goncalo Clemente, Thomas D'huys, Torsten Ruest, Juozas Domarkas, James Thompson, Dominique Schols, Timothy Hubin, Chris Cawthorne and Stephen Archibald

J Nucl Med.

Published online: June 14, 2019.

Doi: 10.2967/jnumed.118.218008

This article and updated information are available at:
<http://jnm.snmjournals.org/content/early/2019/06/14/jnumed.118.218008>

Information about reproducing figures, tables, or other portions of this article can be found online at:
<http://jnm.snmjournals.org/site/misc/permission.xhtml>

Information about subscriptions to JNM can be found at:
<http://jnm.snmjournals.org/site/subscriptions/online.xhtml>

JNM ahead of print articles have been peer reviewed and accepted for publication in *JNM*. They have not been copyedited, nor have they appeared in a print or online issue of the journal. Once the accepted manuscripts appear in the *JNM* ahead of print area, they will be prepared for print and online publication, which includes copyediting, typesetting, proofreading, and author review. This process may lead to differences between the accepted version of the manuscript and the final, published version.

The Journal of Nuclear Medicine is published monthly.
SNMMI | Society of Nuclear Medicine and Molecular Imaging
1850 Samuel Morse Drive, Reston, VA 20190.
(Print ISSN: 0161-5505, Online ISSN: 2159-662X)

© Copyright 2019 SNMMI; all rights reserved.

The logo for the Society of Nuclear Medicine and Molecular Imaging (SNMMI) consists of the letters 'S', 'N', 'M', and 'I' arranged in a 2x2 grid. Each letter is white and set within a red square. To the right of this grid, the text 'SOCIETY OF NUCLEAR MEDICINE AND MOLECULAR IMAGING' is written in a black, sans-serif font, stacked in three lines.
SOCIETY OF
NUCLEAR MEDICINE
AND MOLECULAR IMAGING